

EFFECT OF HEAT TRANSFER ON TAR AND LIGHT GASES FROM COAL PYROLYSIS

J. D. Freihaut, W. M. Proscia, D. J. Seery

United Technologies Research Center
East Hartford, CT 06108

INTRODUCTION

Recent evidence has demonstrated that the products of coal pyrolysis vary with the conditions of heating. Both the reactivity of the char and the chemical composition of the evolved species vary with thermal flux during pyrolysis. Because of the inherent complexity of coal, it is difficult to uncouple the actual heat transfer process and the effects of variations in individual parameters in most pyrolysis experimental designs. Typical ranges of heat transfer rates available in a number of devolatilization reactor systems are indicated in Fig. 1. A particular reactor system may have additional constraints imposed by the nature of the heat flux source or transfer media - acceptable particle size of the parent coal, ambient pressure in which devolatilization can be performed, spectral distribution of a radiant source, residence time in the heat transfer field, etc. Some practical size constraints of wire grid and entrained flow reactor systems are noted in Figure 1.

This report presents the results of a study of coal pyrolysis in three different reactors covering a wide range of heating conditions. The specific purpose of the investigation was to determine if the rate of heat delivery to a high volatile bituminous coal during the tar formation and evolution phase has a significant effect on the tar yields and molecular weight distribution for a high volatile bituminous coal. From the point of view of understanding coal devolatilization and the development of fundamental kinetic models, the investigation is geared to determining whether the same tar formation and evolution processes are occurring in widely different regimes of heat transfer rate and modes of heat transfer. The heavy hydrocarbons yields and chemical characteristics provide a type of observable monitor, to generate a microscopic model of the devolatilization/pyrolysis process.

EXPERIMENTAL

Reactor Characterization

The influence of transport on coal devolatilization necessitates the characterization of reactor heat transfer properties in detail. Figure 1 displays the power density regimes required for a given heating rate of inert, spherical particles having thermal capacities equivalent to coal. Also shown are the range of power density capabilities of the heated grid and flash lamp reactors employed in this investigation and the corresponding regimes for entrained flow reactors. The heated grid system employed in this investigation generates power densities of 1-6 watts/cm² at grid temperatures between 600°K and 1200°K. The flash lamp system generates power densities, in the form of transient irradiance levels. Time averaged levels from 200 watts/cm² to greater than 700 watts/cm² were employed. Entrained flow reactors generally operate in the 10-100 watts/cm² regime. Final particle

temperatures of 1000°K or greater can be obtained in each system, but for significantly different transient times.

UTRC Heated Grid (HG)

The heated grid experiments are conducted by imposing a controlled voltage across a folded No. 325 mesh stainless steel screen. The screens are prefired, then loaded with 20-30 mg of coal by evenly distributing the coal between the folds of the screen. Simultaneous, real time measurements of applied voltage across the screen, current flow, and temperature of the screen are made by a rapid data acquisition system. The grid, char and tar are quenched by impingement of high velocity helium jets on the grid at the end of the heating program. The light gases evolved are measured by a FT-IR gas analysis system attached directly to the heated grid cell. Details of the UTRC heated grid apparatus have been given previously (Ref. 1, 2). The power density fields in vacuum conditions consist mainly of irradiance, whereas in the presence of ambient gases there can be significant gas conduction depending on the thermal conductivity of the gas. The power density fields were determined by synchronously measuring delivered current and voltage while measuring the temperature of the screen at pseudo steady-state conditions, and normalizing with respect to screen surface area. Depending on the heat transfer and heat capacity properties of the sample relative to the screen and ambient gas, the sample can couple to the local power density field. Such coupling has been demonstrated to change the observed temperature trajectory of the screen relative to an unloaded screen area (Ref. 1, 2). The main element of interest is the magnitude of the power density levels established by the heated grid system in the 600°K to 1000°K screen temperature regime, the temperatures of tar formation and evolution in such heating systems (Refs. 3, 4, 5).

UTRC Flash Lamp (FL)

Details of the flash lamp reactor have been given previously (Ref. 6). Under the range of capacitor voltage levels used in this investigation and with the particular match of lamp characteristics and driving circuit parameters the shape of the pulse did not vary significantly. The magnitude of the irradiance level delivered to the inside of the reactor was controlled by varying the neutral density filter and/or the capacitor bank voltage levels. The real time irradiance levels of the flash pulse were monitored by fast response pyroelectric detectors. The detectors employed were calibrated with NBS irradiance standard lamps and a NBS traceable radiometer system used in conjunction with a chopped Argon ion laser. Pyroelectric detectors have a nearly constant response to wavelength from the UV to IR spectral regimes. Because of the possibility of inducing photochemical reactions with the UV component of the flash pulse, the reactors employed were pyrex, as were the neutral density filters. The delivered radiation is characterized by wavelengths ranging from 0.4 to 2.0 microns with peak intensities between 0.8 and 1.1 microns.

Entrained Flow Reactor (EF)

In the entrained flow reactor, coal is entrained in a primary gas and injected into a hot wall furnace, through which a preheated secondary gas is flowing whose temperature is matched with the wall. Entrained coal/char particles flow in a pencil-like stream down the center of the furnace tube and

are collected by a water cooled probe. Figures 2, 3 and 4 display the overall reactor design, aerosol-char separation device and the aerosol and char separation trains. Approximately 75% of the total reactor flow is diverted to the aerosol train. Both the cyclone (char) train and impactor (aerosol) train are followed by final filters. These filters consist of porous metal disks to ease in removal of tar species. Approximately 90% of the tar mass appears to collect on the final filters, with some deposition on stages 7 and 8 of the impactor train. SEM analysis of the impactor and cyclone stages as well as the final filters reveal the phase separator extracts particulates and aerosols less than 2 microns from the particulate flow at 75% gas flow removal. Tar material deposited on the final filter substrates consists almost entirely of condensed heavy hydrocarbons having no particulate boundary structure. Particulate material is efficiently removed by the impactor and cyclone stages.

Because the coals were initially size separated by aerodynamic means, it was originally thought that the size specific ASTM ash could be used as the basis for calculating mass fraction loss via the ash tracer technique. However, using this value gave negative weight loss results for the low wall temperature runs. Inspection of the gas analysis system data and the filter stages of the cyclone and impactor trains indicated substantial devolatilization was occurring. It became apparent that the feed system was not delivering coal particles having the same average ash content as measured for the gross sample for this particular size cut. Consequently, the reactor system was operated in the cold wall, cold flow mode with the delivered coal particles collected in stage 0 of the cyclone separator considered as representative of the actually delivered samples. It was noted that immeasurably small samples of fines were deposited in the impactor train or subsequent stages of the collection system.

Tar Sampling and Handling

Tar yields in the heated grid reactor are determined by weighing the condensable material deposited on the inside of the reactor walls and filters placed between the reactor and FT-IR gas cell. Tar yields in the flash lamp reactor are defined as the THF soluble portion of the condensibles found inside the reactor and on the filters placed between the reactor and FT-IR gas cell. These tars may contain material extracted from char particles in addition to "desorbed" (vaporized molecules, ejected molecular clusters and colloidal fragments) species evolved in the flash heating process. Relative molecular weight distributions of tars were determined with the THF soluble (room temperature, ten minute ultrasonic bath) portion of the evolved species. Entrained flow reactor tars were defined as the THF soluble portion of the material removed from the filtering system. All samples were passed through a 0.5 micron filter before injection into the SEC system. The details of the SEC have been given previously (Ref. 7).

RESULTS AND DISCUSSION

Tar yields and relative molecular weight distributions were obtained for PSOC1451. The elemental analysis for the mesh and aerodynamically separated coal samples are given in Table Ia. Table Ib lists the elemental compositions observed for the 20 - 30 micron cut of the parent coal PSOC 1451 D sample, the delivered particles captured in stage 0 of the cyclone collector, and the residual particles remaining in the feeder bed after several runs. Obviously,

the feed system delivers 20 - 30 micron particles having lower average mineral densities than that observed for the gross parent sample. The residual particles, that is, the particles left in the feeder bed have higher average mineral densities than the gross parent sample. Despite the fact that the size separation system and the feeder system both employ aerodynamic principles, segregation does occur in the reactor feed process. As a result it was deemed necessary to perform cold flow runs with each sample to generate baseline ash data for determining mass reaction yields by ash tracer calculations. Results for tar yields, number average (Mn), and weight average (Mw) molecular weights are summarized in Table II. The data have been arranged in order of increasing net power density. The incident power density has been estimated from reactor property measurements indicated above and heat balance calculations assuming coal particles are spherical, with emissivity and absorptivity of 0.9, and heat capacity of 0.3 cal/gm-C. The particle sizes listed are an arithmetic average diameter of the high and low cutoff of the mesh range. The entrained flow tar yields are estimates based on one atmosphere runs performed in the flash lamp and heated grid reactor where particles were heated to the same final temperatures.

The limits of the molecular weight distributions range from 100-3500 for the heated grid and entrained flow tars, and from 100-5000 for the flash lamp tars. Previous investigators have obtained similar results for average molecular weights and for the range of the MWD's of various coal tars, and coal extracts (see Table III).

Pressure Effect in a Particular Reactor

Heated grid and flash lamp experiments were conducted at atmospheric and low pressures. The entrained flow reactor was operated at one atmosphere only. Comparisons of heated grid and flash lamp data given above (Table II) reveal a highly coupled dependency between mass and heat transfer parameters in determining molecular weight characteristics of the evolved tars. Larger MWD moments are obtained with the heated grid apparatus under low pressure conditions relative to atmospheric pressure for a given power program input (Fig. 5). The low pressure tars obtained in this apparatus have a significantly larger fraction of high MW species than the corresponding atmospheric pressure tars. Tar yields are reduced by 30% or more, depending on specific conditions, while molecular weight moments are reduced. These results are consistent with the results of Unger and Suuberg (Ref. 8) and others (Ref. 9, 10).

The same MWD pattern emerges at the lowest power density inputs employed with the flash lamp apparatus. That is, the low pressure tars have significantly higher molecular weight moments than the corresponding tars formed in one atmosphere of helium or argon (Fig. 5). However, at the next highest irradiance level (285 w/cm²) the tars formed in one atmosphere of helium have larger moments than the corresponding low pressure conditions. These results can be understood relative to the variation in heat transfer conditions. Particles subject to a radiant pulse in low pressure conditions can only cool by an ablative process whereas particles radiantly heated in the presence of an ambient gas are cooled by conduction across a boundary layer as the particle temperature rises. In low pressure conditions the tars formed within the heating particle become hot enough to undergo some secondary cracking reactions in the evolution process. Depending on its thermal conductivity, the moderating influence of the ambient gas can be appreciable,

resulting in a lowering of the net power density delivered to the particles. Consequently, the lowest irradiance level employed was not sufficient to heat the 50 micron particles, in the presence of helium, to desorb more than 5 to 10% of the coal mass as tars. In vacuum conditions, on the other hand, the observed tar yield was ~23% for the lowest irradiance level. In one atmosphere of argon the yield was ~19% with MWD moments similar but somewhat lower than the corresponding vacuum run. The results also indicate that the change in irradiance level from an average level of 225 w/cm² to 285 w/cm² in low pressure conditions results in thermal cracking reactions of the tars as they are evolving from the correspondingly hotter particles. Light gas - CH₄, CO, C₂H₂, C₂H₄, HCN-yields associated with such high temperature reactions of tars are also increased. Although increases in CH₄ and CO are observed in the heated grid gas yields when the tar evolution process is performed in pressure as opposed to vacuum, significant changes in C₂H₂ and HCN are not observed for this coal type with a change in ambient pressure alone.

Variation in Molecular Weight Distributions with Power Density Level

The influence of power density on tar yields and MWD's was explored by utilizing the multi-reactor approach discussed previously. The effect of large differences in power density is explored by comparing results from different reactors for a particular ambient gas environment (Figure 6). The heated grid tars, which were devolatilized at the lowest incident power fields are observed to have lower number average and weight average molecular weights than the flash lamp tars, devolatilized at the highest power densities. The main mode of energy transfer is radiation in these reactors when operated in low pressure conditions, although the wavelength distribution of the radiation is shifted to the visible and near IR for the flash lamp relative to the heated grid. The molecular weight moments of the entrained flow reactor tars vary substantially with residence time. In order to compare results to the other reactors, the shortest residence time tars should be examined since these presumably will have experienced the smallest degree of gas-phase secondary reactions. The tars produced in the 900°C, 40 msec residence time conditions have slightly lower molecular weights than the atmospheric pressure heated grid tars while the 1000°C, 40 msec tars show similar moment characteristics. In both cases the initial tars (low residence time) show molecular weight moments less than the vacuum tars formed in the heated grid. Relative to the flash lamp tars generated in either vacuum or pressure conditions the EF reactor tars have lower moment and distribution characteristics.

Devolatilization Modeling and Coal Structure

For a given set of heat transfer conditions and particle size, it can be difficult to distinguish between mass and heat transfer effects on volatiles product distributions and characteristics (Ref. 11). Both phenomena can appear to effect any one observable similarly by introducing intraparticle or extra-particle (particle-gas boundary layer or entrainment stream) secondary reactions in evolving tar species. Lumped parameter measurements - tar yield, char yield, gas yield, weight loss - are not informative and can even be misleading for a microscopic understanding of coal devolatilization. Kinetic comparisons based on one yield characteristic or product type grossly oversimplify the complexity of the process and can be even more misleading. The results reported in this investigation indicate that detailed

characteristics of tar species generated under one set of reactor conditions can give more insight into the devolatilization process, but only if careful consideration of reactor conditions are included and detailed comparisons are made to results obtained with other reactors on the same analytical bases. A combination of tar characteristics and light gas yields and composition for a wide range of reactor conditions are necessary before a comprehensive understanding of coal devolatilization can be established.

The significant change in relative MWD's of desorbed tars with heat transfer rate in low pressure conditions strongly implies a wide distribution of bonding types, ranging from predominantly physical association to covalent bonding, among a wide distribution of organic structure sizes, molecular to colloidal. The "tar" characteristics depend on the rate (power density field) at which thermal energy is delivered to the organic matrix, the mode of energy delivery and mass transport conditions. Such behavior is not unlike that exhibited by large, thermally labile organic molecules which are observed to desorb from a given substrate intact, via pyrolysis fragmentation, or in both forms, depending on the specific mass and heat transfer conditions and the nature of the molecular interactions between the adsorbed molecules and substrate (Ref. 12-19). From a devolatilization perspective high volatile bituminous coals behave as if they contain a wide range of organic structures, molecular and colloidal, attached to a polymeric-like substrate by a variety of physical and chemical bonding types. The presence of specific fractions of physically and chemically bonded species has been postulated to interpret the plastic behavior and generation of intraparticle pyridine extratables during the rapid heating of an Appalachian provide high volatile bituminous coal (4, 40). The size characteristics of the desorbed species varies depending on whether pyrolysis fragmentation or desorption of relatively large species is emphasized by the heating conditions employed in devolatilization as well as mass transport related parameters.

Acknowledgements

The authors are grateful to Dr. D. Maloney for providing tar samples for comparisons. D. Santos and G. Wagner provided critical technical assistance in carrying out this investigation. Partial funding was provided by the Department of Energy under Contract DE-AC22-84PC70768.

TABLE Ia

PSOC 1451 (HVA BIT - Appalachian Province)
Elemental Composition

Mesh <d>	-270+325 49	-100+140 127	-50+70 254	-25+35 604	-20+25 774
%DAF					
C	82.38(0.47)*	82.26(0.36)	82.28(0.36)	80.66(2.80)	78.40(4.87)
H	5.44(0.03)	5.54(0.03)	5.58(0.02)	5.71(0.28)	5.69(0.20)
N	1.60(0.03)	1.62(0.02)	1.63(0.01)	1.56(0.08)	1.52(0.14)
S+O	10.58(0.55)	11.10(0.45)	10.48(0.37)	12.26(3.30)	14.13(4.83)
Ash	5.89(0.55)	10.78(0.69)	9.11(1.32)	24.39(18.9)	32.50(29.6)

* Numbers in parentheses represent one standard deviation.

<d> = Arithmetic average of particle range in microns

TABLE Ib

ELEMENTAL COMPOSITION OF PARENT, DELIVERED AND RESIDUAL PARTICLES:
PSOC 1451D, 20 - 30 MICRON PARTICLES

SAMPLE	%C	%H	%N	%S+O	%ASH*
PARENT-1	75.19	4.94	1.48	9.66	8.69
PARENT-2	75.25	4.95	1.45	9.52	8.80
PARENT-3	75.00	4.91	1.45	9.82	8.80
PARENT-4	75.06	4.90	1.45	9.78	8.80
DELIVERED-1	78.49	5.08	1.53	10.08	4.80
DELIVERED-2	78.54	5.08	1.50	10.36	4.50
DELIVERED-3	78.56	5.12	1.51	10.09	4.69
DELIVERED-4	78.59	5.08	1.48	10.01	4.80
RESIDUAL-1	74.46	4.91	1.41	9.49	9.69
RESIDUAL-2	74.42	4.89	1.43	9.84	9.39
RESIDUAL-3	74.45	4.90	1.45	9.99	9.19
RESIDUAL-4	74.44	4.91	1.45	9.78	9.39

TABLE II

TAR YIELDS AND MOLECULAR WEIGHTS

REACTOR/ PARAMETERS	PARTICLE SIZE [m]	ATM.	POWER DENSITY [W/CM ²]	Mn	Mw	% TAR YIELD	RUN I.D.
HG 450/2 *	49	VAC	0.62	626	839	14.2	229B
HG 550/2	49	AR	0.74	510	703	14.9	238A
HG 600/10	49	VAC	0.88	594	775	25.1	239A
HG 550/2	49	VAC	0.94	664	960	35.3	232C
HG 600/10	49	HE	1.3	522	692	12.7	242A
HG 350/1	49	VAC	1.8	655	948	20.0	224B
HG 800/2.5	49	VAC	1.9	621	855	21.0	221A
HG 800/2.5	49	VAC	1.9	610	843	24.4	237B
HG 800/2.5	254	VAC	2.0	639	869	25.1	246A
HG 800/2.5	127	VAC	2.1	616	841	28.4	245A
HG 800/2	774	VAC	2.3	616	875	24.3	253A
HG 800/2.5	774	VAC	2.3	632	869	23.3	247A
HG 800/2.5	49	AR	2.3	520	734	17.5	235C
EF 900/3 **	64	N2	50.0	485	698	****	017
EF 900/9	64	N2	-	490	709	-	018
EF 900/22	64	N2	-	382	560	-	019
EF 1000/3	64	N2	80.0	531	766	****	020
EF 1000/9	64	N2	-	406	596	-	021
EF 1000/22	64	N2	-	275	407	-	022
FL 1.8/30 ***	49	HE	225(32)	686	1059	6.0	705J
FL 1.5/60	49	HE	285(40)	784	1184	12.0	703C
FL 1.5/90	49	HE	430(60)	699	1134	19.0	704B
FL 2.2/60	49	HE	730(96)	545	898	17.0	706E
FL 1.8/30	49	AR	225(122)	714	1121	19.0	707C
FL 1.8/30	49	VAC	225	764	1180	23.0	709B
FL 1.5/60	49	VAC	285	663	1054	28.4	713B
FL 2.2/60	49	AR	729(293)	630	955	22.0	708B

Footnotes:

* HG X/Y - heated grid with 1000 C/sec ramp to X C, hold for Y sec, then 1000^o C/sec ramp to 800^o C, hold for 2.5-Y sec. The 600/10 runs are an exception: ramp to 600^o C and hold for 10 sec.

** EF X/Y - entrained flow with X C gas temperature and Y" sampling position
900^o C: 3"- 40 msec; 9" - 110 msec; 22" - 250 msec
1000^o C: 3"- 40 msec; 9" - 100 msec; 22" - 230 msec

*** FL X/Y - flash lamp with X KV capacitor bank voltage and Y% neutral density filter. Values are time-averaged delivered irradiance; values inside parentheses are time-averaged net power density calculated from heat balance considerations. See Table III for characteristics of flash pulses.

**** - Not measured directly; at 3" residence time is estimated be about 20% (daf) of the parent coal mass from heated grid and flash lamp investigations. This yield represents the major fraction of the total volatile yields (Ref. 25) in 40 msec.

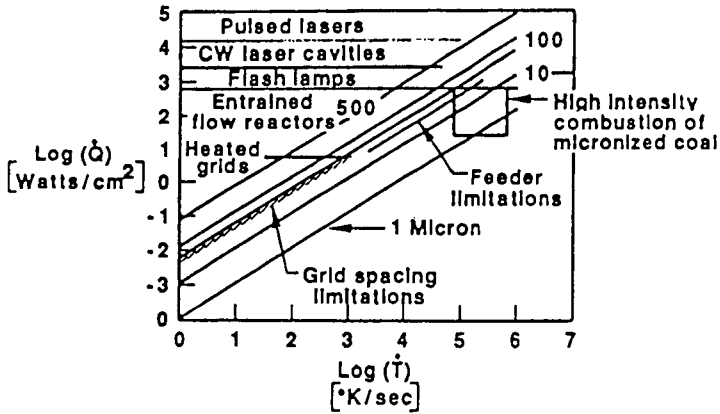
TABLE III
COMPARISON OF MOLECULAR WEIGHTS OF COAL DERIVED COMPOUNDS

SAMPLE	TECHNIQUE	Mn	Mw	MWD RANGE	INVESTIGATOR(S)
Pitt #8	SEC THF				this work
1 atm HG tar		500-525	675-750	100-3500	
vac HG tar		575-675	775-975	100-3500	
EF tar		275-550	400-775	100-3500	
1 atm FL tar		550-800	900-1200	100-5000	
vac FL tar		650-775	1050-1200	100-5000	
<hr/>					
Pitt #8	SEC/VPO pyridine				Oh (1985)
HG tars:					
1 atm		350	-	100-1200	
vac		400	-	100-1200	
HG char extracts:					
1 atm		450	-	100-1500	
vac		500	-	100-1500	
<hr/>					
Pitt Bruceton	SEC/VPO THF				Unger & Suuberg (1984)
HG tars:					
1 atm		500-700	-	100-4000	
vac		750-900	-	100-4000	
HG 1 atm char extracts:		750-1000	-	100-4000+	
<hr/>					
Pitt #8 CO2 laser	SEC				Ballantyne et al. (1983)
1 atm tar	THF	223?	394?	60-3000	
<hr/>					
Low Beam Shaw 84.2% C 115°C pyridine raw coal extract	Ebullio- scopy pyridine	870	-	-	Dormans & van Krevelen (1960)

REFERENCES

1. Freihaut, J.D., Zabielski, M.F. and Seery, D.J., Nineteenth Symposium (Int'l.) on Combustion, The Combustion Institute, 1159 (1982).
2. Freihaut, J.D. and Seery, D.J., ACS Div. of Fuel Chem., Preprints, 27, No. 2, 89 (1982).
3. Howard, J.B. in Chemistry of Coal Utilization, Sec. Supp. Vol. (ed. by Elliott, M.A.), John Wiley and Sons, New York, 340ff (1981).
4. Fong, W.S., Khalil, Y.F., Peters, W.A. and Howard, J.B., Fuel, 65, 195 (1986).
5. Suuberg, E.M., et al., Seventeenth Symposium (Int'l.) on Combustion, The Combustion Institute, Pittsburgh, 117 (1979).
6. Freihaut, J.D. and Seery, D.J., Proceedings of the International Conference on Coal Science, IEA, 957 (1985).
7. Freihaut, J. D., Proscia, W. M. and Seery, D. J. Proceedings of the Third Annual Pittsburgh Coal Conference, 684 (1986).
8. Unger, P.E., and Suuberg, E.M., Fuel, 63, 606 (1984).
9. Oh, M.S., Ph.D. Thesis, M.I.T., Cambridge, MA, 1985.
10. Solomon, P.R., Squire, K.R., and Carangelo, R.M., Proceedings of the International Conference on Coal Science, IEA, 945 (1985).
11. Kaiser, M., Wanzl, W., van Heek, K.H. and Juntgen, H., Proceedings of the International Conference on Coal Science, IEA, 899 (1985).
12. Cotter, R.J., Analytical Chemistry, 52, No. 14, 1589A.
13. Van der Peyl, G.J.Q., Haverkamp, J. and Kistemaker, P.G., Internat. Jnl. of Mass Spectrometry and Ion Physics, 42, 125 (1982).
14. Beuhler, R.J., Flanigan, E., Greene, L.J. and Friedman, L., J. Amer. Chem. Society, 96, No. 12, 3990 (1974).
15. Heresch, F., Schmid, E.R. and Huber, J.F.K., Anal. Chem., 52, 1803 (1980).
16. Posthumus, M.A., Kistemaker, P.G. and Meuzelaar, H.L.C., Analytical Chemistry, 50, No. 7, 985 (1978).
17. Cotter, R.J., Analytical Chemistry, 52, 1770 (1980).
18. Stoll, R. and Rollgen, F.W., Org. Mass. Spec., 14, No. 12, (642) (1979).
19. Kistemaker, P.G., Lens, M.M.J., Van der Peyl, G.J.Q., and Boerboon, A.J.H., Adv. in Mass Spectrometry, 8A, 928 (1980).

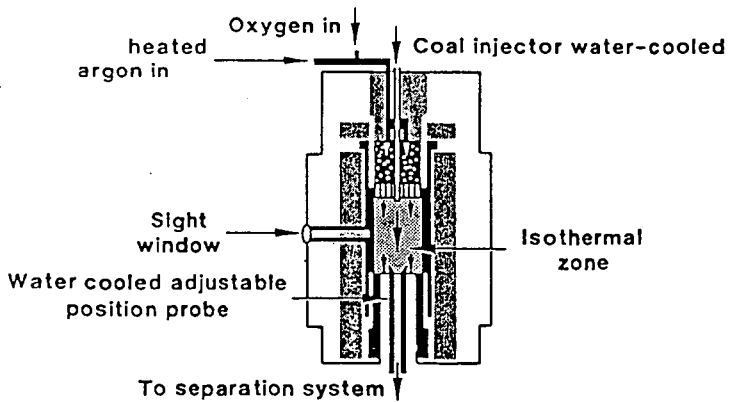
Fig. 1 Reactor Heat Transfer Regimes



841147L41

FIGURE 2

ENTRAINED FLOW REACTOR FOR COAL DEVOLATILIZATION



841147L51

FIGURE 3

AEROSOL - CHAR SEPARATION APPARATUS

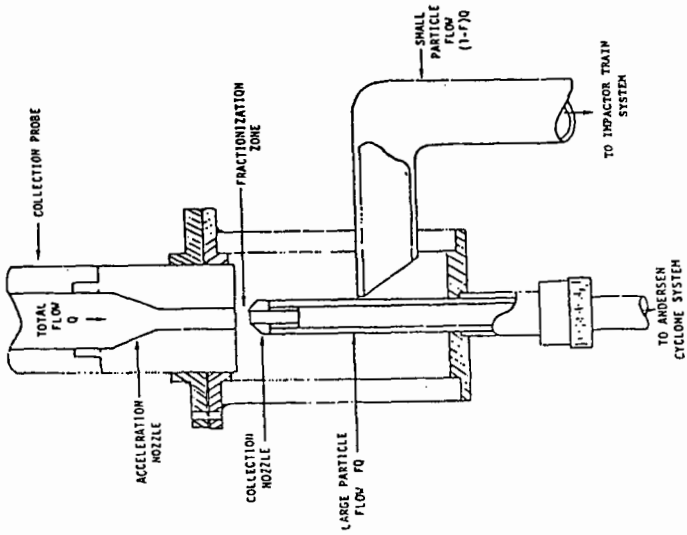


FIGURE 4

SAMPLE COLLECTION SYSTEM

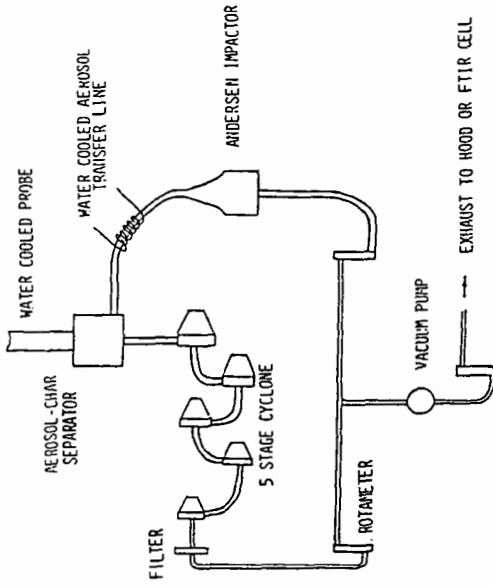


FIG. 5

EFFECT OF PRESSURE On tar molecular weight distributions

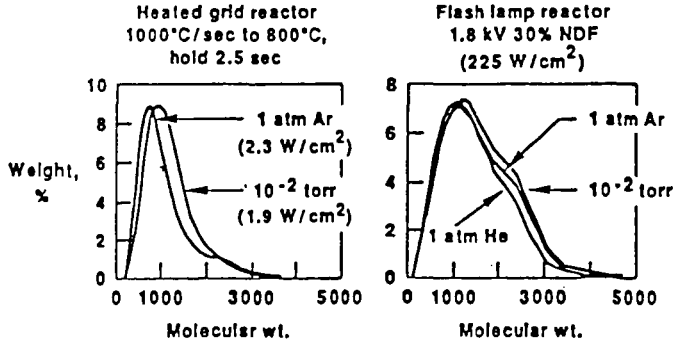


FIG. 6

EFFECT OF DIFFERENT REACTORS On tar molecular weight distributions

